

# DDVCS on nucleons and nuclei

B.Z. Kopeliovich,<sup>\*</sup> Ivan Schmidt,<sup>†</sup> and M. Siddikov<sup>‡</sup>

*Departamento de Física, Centro de Estudios Subatómicos, y Centro Científico - Tecnológico de Valparaíso,  
Universidad Técnica Federico Santa María, Casilla 110-V, Valparaíso, Chile*

In this paper we evaluate the double deeply virtual Compton scattering on nucleons and nuclei in the framework of the color dipole model. Both the effects of quark and the gluon shadowing are taken into account.

PACS numbers: 13.60.Fz, 24.85.+p, 12.40.-y

Keywords: Double deeply virtual Compton scattering, color dipole model

## I. INTRODUCTION

Compton scattering,  $\gamma^* + p \rightarrow \gamma + p$ , with initial photons real or virtual, has been intensively investigated theoretically and experimentally [1–17]. In the case of deeply-virtual Compton scattering (DVCS), where the initial photon is highly-virtual, the QCD factorization has been proven [5, 8, 9] and the amplitude can be expressed in terms of the generalized parton distributions (GPD) [1–6, 8–16] convoluted with some hard coefficient function. However, it is not possible to make a deconvolution and unambiguously extract the GPDs of the target from the experimental DVCS data. The standard procedure in this case is to construct a plausible model with some free parameters, fix the free parameters from the experimental data and after that make conclusions about the GPDs of the target.

The situation is different in case of double deeply virtual Compton scattering (DDVCS),  $\gamma^* + p \rightarrow \gamma^* + p \rightarrow \bar{l}l + p$  [18–20]. As it has been shown in [18], the DDVCS amplitude allows such a deconvolution. Unfortunately, the corresponding cross-section of the process is suppressed by  $\alpha_{em}/3\pi$  compared to ordinary DVCS and falls into a picobarn-level range, so it cannot be accessed by the existing accelerating facilities. However, at future accelerating facilities [21, 22] with higher luminosities, this cross-section can be measured. A special case, when the initial photon is real, has been studied in [23, 24], and in the color dipole framework in [25]. This process may be viewed as time-inverted DVCS with negative virtuality  $-M_{ll}^2$ , so the color dipole model is applicable for high lepton masses,  $M_{ll}^2 \gg M_N^2$ . A high luminosity flux of real photons may be created by ultraperipheral scattering of protons on nuclei; such collisions at the LHC will be an ideal tool for the study of this process. However, it is not possible to access the whole DDVCS amplitude in ultraperipheral hadronic collisions, since the virtuality of the initial photon, controlled by the formfactors of the colliding hadrons, cannot be very high. Thus, the only way to study the DDVCS is the electroproduction of lepton pairs,  $e + p \rightarrow e + p + \bar{l}l$ .

Recently DVCS on proton and nuclear targets has been studied within the color dipole approach in [26–30]. In this paper we extend that study to the DDVCS case. We focus on the high-energy kinematics range, since the future accelerating facilities are expected to operate at these energies [21, 22], where the effects of coherence are important. The general framework for evaluating the shadowing corrections is the Gribov-Glauber approach [31, 32]. In particular, we take into account gluon shadowing corrections, which correspond to the triple-Pomeron diffraction in the Gribov inelastic shadowing corrections. These corrections onset at  $x_B \lesssim 10^{-2}$ , and give a sizeable contribution to nuclear shadowing at  $x_B \sim 10^{-5}$ .

The paper is organized as follows. In Sections II we review the general formalism of the color dipole approach. In Section III we discuss the frequently used frozen approximation, which is valid for asymptotically large energies. In Section IV we discuss the method which will be used for calculations of nuclear shadowing effects and demonstrate that for asymptotically large energies it reproduces the results from Section III. In Section V we discuss the gluon shadowing and its effect on the DDVCS observables. In Section VI the wavefunction of a real photon is evaluated in the instanton vacuum model. In Section VII we present the results of numerical evaluation and draw conclusions.

---

<sup>\*</sup>Electronic address: Boris.Kopeliovich@usm.cl

<sup>†</sup>Electronic address: Ivan.Schmidt@usm.cl

<sup>‡</sup>Electronic address: Marat.Siddikov@usm.cl

## II. COLOR DIPOLE MODEL

The electroproduction cross-section for unpolarized lepton pairs in the DDVCS process has a form

$$\frac{d\sigma^{\bar{l}lp}}{dt dM_{ll}^2} = \frac{d\sigma_{el}^{\gamma p}}{dt} \frac{\alpha_{em}}{3\pi M_{ll}^2} \left(1 - \frac{4m_l^2}{M_{ll}^2}\right)^{3/2}, \quad (1)$$

where  $d\sigma_{el}^{\gamma p}/dt$  is the cross-section of the process  $\gamma^*p \rightarrow \gamma'^*p$ ,  $M_{ll}^2$  is the invariant mass of the produced lepton pair, and  $t$  is the square of the momentum transferred to a target. In what follows, we will concentrate on evaluation of the cross-section  $d\sigma_{el}^{\gamma p}/dt$ . For the unpolarized Compton scattering discussed in this paper we obtain,

$$\frac{d\sigma_{el}^{\gamma p}}{dt} = \frac{1}{16\pi} \sum_{ij} \left| \mathcal{A}_{\mu\nu}^{(ij)} \right|^2, \quad (2)$$

where the amplitude  $\mathcal{A}_{\mu\nu}^{(ij)}$  is evaluated in the color dipole model. In this model the dominant contribution to the Compton amplitude comes from gluonic exchanges. Then the general expression for the Compton amplitude on a nucleon has the form,

$$\mathcal{A}_{\mu\nu}^{(ij)}(s, \Delta, Q^2, M_{ll}^2) = e_\mu^{(i)} e_\nu^{(j)} \int_0^1 d\beta_1 d\beta_2 d^2r_1 d^2r_2 \bar{\Psi}_f^{(i)}(\beta_2, \vec{r}_2) \mathcal{A}^d(\beta_1, \vec{r}_1; \beta_2, \vec{r}_2; \Delta) \Psi_{in}^{(j)}(\beta_1, \vec{r}_1), \quad (3)$$

where  $e_\mu^{(i)}$  is the photon polarization vector;  $\beta_{1,2}$  are the light-cone fractional momenta of the quark and antiquark,  $\vec{r}_{1,2}$  are the transverse distances in the final and initial dipoles respectively;  $\Delta$  is the momentum transfer in the Compton scattering,  $\mathcal{A}^d(\dots)$  is the scattering amplitude of the dipole on the target (proton or nucleus), and  $\Psi_{in(f)}^{(i)}(\beta, \vec{r})$  are the light-cone distribution functions of the initial and final photons in the polarization state  $i$ . When the virtuality of the corresponding photon is large, we may use the well-known pQED expressions [33, 34],

$$\bar{\Psi}_f^{(i)} \Psi_{in}^{(j)} \sim ((\alpha^2 + (1-\alpha)^2) \epsilon_1 \epsilon_2 K_1(\epsilon_1 r) K_2(\epsilon_2 r) + m_q^2 K_0(\epsilon_1 r) K_0(\epsilon_2 r)),$$

where  $\epsilon_i = \sqrt{Q_i^2 \alpha(1-\alpha) + m_q^2}$ , and make an analytical continuation of the space-like wave functions to the time-like photons by a simple extrapolation,  $Q^2 \rightarrow -M_{ll}^2$  [35], and use

$$K_0(ix) = -\frac{i\pi}{2} (J_0(x) - iY_0(x)), \quad (4)$$

$$K_1(ix) = -\frac{\pi}{2} (J_1(x) - iY_1(x)), \quad (5)$$

where  $x = r\sqrt{M_{ll}^2 \alpha(1-\alpha) + m_q^2}$  for the kinematics  $M_{ll}^2 \gg m_q^2/(\alpha(1-\alpha))$ . However when the virtualities are small, we have to resort to some model (see Section VI for more details).

At high energies in the small angle approximation,  $\Delta/\sqrt{s} \ll 1$ , the quark separation and fractional momenta  $\beta$  are preserved, so

$$\mathcal{A}^d(\beta_1, \vec{r}_1; \beta_2, \vec{r}_2; Q^2, \Delta) \approx \delta(\beta_1 - \beta_2) \delta(\vec{r}_1 - \vec{r}_2) \int d^2b' e^{i\vec{\Delta} \cdot \vec{b}'} \Im m f_{\bar{q}q}^N(\vec{r}_1, \vec{b}', \beta_1) \quad (6)$$

$$\begin{aligned} \Im m f_{\bar{q}q}^N(\vec{r}, \vec{b}', \beta) &= \frac{1}{12\pi} \int \frac{d^2k d^2\Delta}{(k + \frac{\Delta}{2})^2 (k - \frac{\Delta}{2})^2} \alpha_s \mathcal{F}\left(x, \vec{k}, \vec{\Delta}\right) e^{i\vec{b}' \cdot \vec{\Delta}} \\ &\times \left( e^{-i\beta \vec{r} \cdot (\vec{k} - \frac{\vec{\Delta}}{2})} - e^{i(1-\beta) \vec{r} \cdot (\vec{k} - \frac{\vec{\Delta}}{2})} \right) \left( e^{i\beta \vec{r} \cdot (\vec{k} + \frac{\vec{\Delta}}{2})} - e^{-i(1-\beta) \vec{r} \cdot (\vec{k} + \frac{\vec{\Delta}}{2})} \right), \end{aligned} \quad (7)$$

where

$$\begin{aligned} \frac{\mathcal{F}(x, \vec{k}, \vec{\Delta})}{k^2} &\equiv H_g(x, \vec{k}, \vec{\Delta}) = \frac{1}{2} \int d^2r e^{ik \cdot r} \int \frac{dz^-}{2\pi} e^{ix \bar{P}^+ z^-} \times \\ &\times \left\langle P' \left| G_{+\alpha} \left( -\frac{z}{2}, -\frac{\vec{r}}{2} \right) \gamma_+ \mathcal{L} \left( -\frac{z}{2} - \frac{\vec{r}}{2}, \frac{z}{2} + \frac{\vec{r}}{2} \right) G^{+\alpha} \left( \frac{z}{2}, \frac{\vec{r}}{2} \right) \right| P \right\rangle \end{aligned} \quad (8)$$

is the gluon GPD of the target,  $P' = P + \Delta$ ,  $\bar{P} = (P + P')/2$ ,  $G_{\mu\nu}(x)$  is the gluon loop operator,  $\mathcal{L}_\infty(x, y)$  is the Wilson factor required by gauge covariance. For this GPD we use a gaussian parameterization [36–38],

$$\mathcal{F}\left(x, \vec{k}, \vec{\Delta}\right) = \frac{3\sigma_0(x)}{16\pi^2\alpha_s} \left(k + \frac{\Delta}{2}\right)^2 \left(k - \frac{\Delta}{2}\right)^2 R_0^2(x) \exp\left(-\frac{R_0^2(x)}{4} \left(\vec{k}^2 + \frac{\vec{\Delta}^2}{4}\right)\right) \exp\left(-\frac{1}{2}B(x)\Delta^2\right), \quad (9)$$

where the phenomenological functions  $\sigma_0(x)$ ,  $R_0^2(x)$ ,  $B(x)$  are fitted to DIS, real photoproduction and  $\pi p$  scattering data. We discuss them in more detail in Section VII. The parameterization (9) does not depend on the longitudinal momentum transfer and decreases exponentially as a function of  $\Delta^2$ . Since the parameterization (9) is an effective one and is valid only in the small- $x$  region, we do not assume that it satisfies general requirements, such as positivity [39] and polynomiality [3] constraints.

The prefactor  $\left(k + \frac{\Delta}{2}\right)^2 \left(k - \frac{\Delta}{2}\right)^2$  in (9) guarantees convergence of the integrals in the parameterization (6). In the forward limit,  $\Delta \rightarrow 0$ , the amplitude (6) reduces to the saturated parameterization of the dipole amplitude proposed by Golec-Biernat and Wüsthoff (GBW) [40],

$$\sigma_d(\beta, r) = 2 \int d^2b' \Im f_{\bar{q}q}^N(\vec{r}, \vec{b}', \beta) = \frac{1}{6\pi} \int \frac{d^2k}{k^4} \alpha_s(k^2) \mathcal{F}\left(x, \vec{k}, \vec{0}\right) = \frac{\sigma_0(x)}{2} \left(1 - \exp\left(-\frac{r^2}{R_0(x)}\right)\right) \quad (10)$$

Generally, the amplitude  $f_{\bar{q}q}^N(\dots)$  involves nonperturbative physics, but its asymptotic behavior for small  $r$  is controlled by pQCD [41]:

$$f_{\bar{q}q}^N(\vec{r}, \vec{\Delta}, \beta)_{r \rightarrow 0} \propto r^2,$$

up to slowly varying corrections  $\sim \ln(r)$ .

The calculation of the differential cross section also involves the real part of scattering amplitude, whose relation to the imaginary part is quite straightforward. According to [42], if the limit  $\lim_{s \rightarrow \infty} \left(\frac{\Im f}{s^\alpha}\right)$  exists and is finite, then the real and imaginary parts of the forward amplitude are related as

$$\Re f(\Delta = 0) = s^\alpha \tan\left[\frac{\pi}{2} \left(\alpha - 1 + \frac{\partial}{\partial \ln s}\right)\right] \frac{\Im f(\Delta = 0)}{s^\alpha}. \quad (11)$$

In the model under consideration the imaginary part of the forward dipole amplitude indeed has a power dependence on energy,  $\Im f(\Delta = 0; s) \sim s^\alpha$ , so (11) simplifies to

$$\frac{\Re \mathcal{A}}{\Im \mathcal{A}} = \tan\left(\frac{\pi}{2}(\alpha - 1)\right) \equiv \epsilon. \quad (12)$$

This fixes the phase of the forward Compton amplitude, which we retain for nonzero momentum transfers, assuming similar dependences for the real and imaginary parts. Finally we arrive at,

$$\mathcal{A}_{\mu\nu}^{(ij)} = (\epsilon + i)e_\mu^{(i)}(q')e_\nu^{(j)}(q) \int d^2r \int_0^1 d\beta \bar{\Psi}_f^{(i)}(\beta, r) \Psi_{in}^{(j)}(\beta, r) \Im f_{\bar{q}q}^N(\vec{r}, \vec{\Delta}, \beta, s), \quad (13)$$

### III. NUCLEAR SHADOWING IN THE FROZEN LIMIT

Nuclear shadowing signals the closeness of the unitarity limit. Hard reactions possess this feature only if they have a contribution from soft interactions. In DIS and DVCS the soft contribution arises from the so called aligned jet configurations [43], corresponding to  $\bar{q}q$  fluctuations very asymmetric in sharing the photon momentum,  $\beta \ll 1$ . Such virtual photon fluctuations, having large transverse separation, are the source of shadowing [49].

Calculation of nuclear shadowing simplifies considerably in the case of long coherence length [44], i.e. long lifetime of the photon fluctuations, when it considerably exceeds the nuclear size. In this case Lorentz time dilation "freezes" the transverse size of the fluctuation during propagation through the nucleus. Then the Compton amplitude of coherent scattering, which leaves the nucleus intact, has the same form as Eq. (13) with a replacement of the nucleon Compton amplitude by the nuclear one,

$$\Im f_{\bar{q}q}^N(r, \beta, \Delta) \Rightarrow \Im f_{\bar{q}q}^A(r, \beta, \Delta) = \int d^2b e^{i\vec{\Delta} \cdot \vec{b}} \left[1 - e^{-\Im f_{\bar{q}q}^N(r, \beta, \Delta=0) T_A(b)}\right], \quad (14)$$

where  $b$  is impact parameter of the photon-nucleus collision,  $T_A(b) = \int_{-\infty}^{\infty} dz \rho_A(b, z)$  is the nuclear thickness function, given by the integral of nuclear density along the direction of the collisions. In this expression we neglect the real part of the amplitude which is particularly small for a coherent nuclear interaction.

For incoherent Compton scattering, which results in nuclear fragmentation without particle production (quasielastic scattering), the cross section has the form [45],

$$\begin{aligned} \frac{d\sigma_{qel}^{\gamma A}}{dt} &= B_{el} e^{B_{el}t} \sum_{ij} \int_0^1 d\beta \int d^2r d^2r' \bar{\Psi}_f^{(i)}(\beta, r) \bar{\Psi}_f^{(i)}(\beta, r') \Psi_{in}^{(j)}(\beta, r) \Psi_{in}^{(j)}(\beta, r') \\ &\times \exp \left[ \frac{1}{2} \left( \sigma_{\bar{q}q}(r) - \sigma_{\bar{q}q}(r') \right) T_A(b) \right] \left\{ \exp \left[ \frac{\sigma_{\bar{q}q}(r) \sigma_{\bar{q}q}(r')}{16\pi B_{el}} T_A(b) \right] - 1 \right\} \\ &\approx \frac{e^{B_{el}t}}{16\pi} \int d^2b T_A(b) \left| \int_0^1 d\beta d^2r \bar{\Psi}_f(\beta, r) \sigma_{\bar{q}q}(r, s) \Psi_{in}(\beta, r) \exp \left[ -\frac{1}{2} \sigma_{\bar{q}q}(r) T_A(b) \right] \right|^2. \end{aligned} \quad (15)$$

Here  $B_{el}$  is the  $t$ -slope of elastic dipole-nucleon amplitude. In this equation we treated the term quadratic in the dipole cross section as a small number and expanded the exponential in curly brackets.

#### IV. ONSET OF NUCLEAR SHADOWING

The regime of frozen dipole size discussed in the previous section is valid only at very small  $x_B$ , or at high energies. However, at medium small  $x_B$  a dipole can "breathe", i.e. vary its size, during propagation through the nucleus, and one should rely on a more sophisticated approach.

In this paper we employ the description of the onset of shadowing developed in [46] and based on the light-cone Green function technique [47]. The propagation of a color dipole in a nuclear medium is described as motion in an absorptive potential, *i.e.*

$$i \frac{\partial G(z_2, r_2; z_1, r_1)}{\partial z_2} = -\frac{\Delta_{r_2} G(z_2, r_2; z_1, r_1)}{\nu\alpha(1-\alpha)} - k_{min} G(z_2, r_2; z_1, r_1) - \frac{i\rho_A(z_2, r_2) \sigma_{\bar{q}q}(r_2)}{2} G(z_2, r_2; z_1, r_1), \quad (16)$$

where the Green function  $G(z_2, r_2; z_1, r_1)$  describes the probability amplitude for the propagation of dipole state with size  $r_1$  at the light-cone starting point  $z_1$  to the dipole state with size  $r_2$  at the light-cone point  $z_2$ , and

$$k_{min} = \frac{Q^2\alpha(1-\alpha) + m_q^2}{2\nu\alpha(1-\alpha)}.$$

Then the shadowing correction to the amplitude has the form

$$\begin{aligned} \delta A(s, \vec{\Delta}_\perp) &= \int d^2b e^{i\vec{\Delta} \cdot \vec{b}_\perp} \int_{z_1 \leq z_2} dz_1 dz_2 \rho_A(b, z_1) \rho_A(b, z_2) \int_0^1 d\alpha d^2r_1 d^2r_2 \times \\ &\bar{\Psi}_f(\alpha, r_2) \sigma_{\bar{q}q}(r_2) G(z_2, r_2; z_1, r_1) \sigma_{\bar{q}q}(r_1) \Psi_{in}(\alpha, r_1). \end{aligned} \quad (17)$$

Equation (16) is quite complicated and in the general case may be solved only numerically [48]. However in some cases an analytic solution is possible. For example, in the limit of long coherence length,  $l_c \gg R_A$ , relevant for high-energy accelerators like the LHC, one can neglect the "kinetic" term  $\propto \Delta_{r_2} G(z_2, r_2; z_1, r_1)$  in (16), and get the Green function in the "frozen" approximation [47],

$$G(z_2, r_2; z_1, r_1) = \delta^2(r_2 - r_1) \exp \left( -\frac{1}{2} \sigma_{\bar{q}q}(r_1) \int_{z_1}^{z_2} d\zeta \rho_A(\zeta, b) \right) e^{ik_{min}(z_2 - z_1)}. \quad (18)$$

Then the shadowing correction (17) simplifies to

$$\delta\mathcal{A}(s, \Delta_\perp) = \int d^2b e^{i\vec{\Delta}_\perp \cdot \vec{b}_\perp} \int_{z_1 \leq z_2} dz_1 dz_2 \rho_A(z_1, b) \rho_A(z_2, b) \int_0^1 d\alpha d^2r \sigma_{\bar{q}q}^2(r, b) \times \bar{\Psi}_f(\alpha, r) \exp\left(-\frac{1}{2}\sigma_{\bar{q}q}(r) \int_{z_1}^{z_2} d\zeta \rho_A(\zeta, b)\right) \Psi_{in}(\alpha, r) e^{ik_{min}(z_2 - z_1)}. \quad (19)$$

If we neglect the real part of the amplitude and the longitudinal momentum transfer  $k_{min}$  (which is justified for asymptotically large  $s$ ), and average over polarizations, then taking the integral over  $z_{1,2}$  "by parts" in (19), we get for the elastic amplitude

$$\mathcal{A}(s, \Delta_\perp) = 2 \int d^2b e^{i\vec{\Delta}_\perp \cdot \vec{b}_\perp} \int_0^1 d\alpha d^2r \bar{\Psi}_f(\alpha, r) \left[1 - \exp\left(-\frac{1}{2}\sigma_{\bar{q}q}(r) \int_{-\infty}^{+\infty} d\zeta \rho_A(\zeta, b)\right)\right] \Psi_{in}(\alpha, r). \quad (20)$$

Another case where an analytical solution is possible is when the effective dipole sizes are small and the function  $\sigma_{\bar{q}q}(r)$  may be approximated as

$$\sigma_{\bar{q}q}(r) \approx Cr^2. \quad (21)$$

This approximation cannot be precise even at high virtualities  $Q^2$  and  $M_l^2$  in DDVCS, since there are contributions of the aligned jet configurations mentioned above, which permit large dipoles even for large virtualities. Moreover, such aligned jet configurations of the dipole provide the main contribution to nuclear shadowing [49]. Nevertheless, for the sake of simplicity we use this approximation in order to *estimate* the magnitude of the shadowing corrections in the region  $x_B \in (10^{-3}, 10^{-1})$ . The approximation (21) is well justified on heavy nuclei. Namely, nuclear shadowing is independent of the form of the dipole cross section for large dipole sizes, above the saturation point,  $r^2 > 4/Q_s^2$ , where the typical value of the saturation momentum is  $Q_s^2 \sim 1 \text{ GeV}^2$  for heavy nuclei. Indeed, in this case the nucleus is "black". Therefore the shape of the dipole cross section matters only at  $r^2 < r_s^2 = 0.16 \text{ fm}^2$ . This size is sufficiently small for using the  $r^2$  approximation (21). Numerically, the approximation (21) was tested in [48]—it was found that the discrepancy between the approximation (21) and the exact numerical solution of (16), changes the nuclear shadowing for DIS only within ten percent. We expect that within the same accuracy the approximation (21) is valid for DVCS.

Then Eq. (16) yields for  $W(z_2, r_2; z_1, r_1)$  the well-known evolution operator of harmonic oscillator, although with complex frequency

$$G(z_2, r_2; z_1, r_1) = \frac{a}{2\pi i \sin(\omega \Delta z)} \exp\left(\frac{ia}{2 \sin(\omega \Delta z)} [(r_1^2 + r_2^2) \cos(\omega \Delta z) - 2\vec{r}_1 \cdot \vec{r}_2]\right) e^{ik_{min}(z_2 - z_1)}, \quad (22)$$

$$\omega^2 = \frac{-2iC\rho_A}{\nu\alpha(1-\alpha)},$$

$$a^2 = -iC\rho_A\nu\alpha(1-\alpha)/2$$

## V. GLUON SHADOWING

It has been known since [50, 51] that in addition to the quark shadowing inside nuclei there is also shadowing of gluons, which leads to attenuation of the gluon parton distributions. While nuclear shadowing of quarks is directly measured in DIS, the shadowing of gluons is poorly known from data [52, 53], mainly due to the relatively large error bars in the nuclear structure functions and their weak dependence on the gluon distributions, which only comes via evolution. The theoretical predictions for gluon shadowing strongly depend on the implemented model—while for  $x_B \gtrsim 10^{-2}$  they all predict that the gluon shadowing is small or absent, for  $x_B \lesssim 10^{-2}$  the predictions vary in a wide range (see the review [53] and references therein). Some of the recent analysis [64] led to such a strong gluon shadowing, that the unitarity bound [65] was severely broken. Since in this paper we also make predictions for the LHC energy range, the gluon shadowing corrections should be taken into account as well.

The attenuation factor  $R_g$

$$R_g(x, Q^2, b) = \frac{G_A(x, Q^2, b)}{T_A(b)G_N(x, Q^2, b)},$$

where  $G_N(x, Q^2, b)$  is the impact parameter dependent gluon PDF, was evaluated in the dipole approach in [54, 55]. It was found convenient to evaluate  $R_g$  relating it to the shadowing corrections in DIS with longitudinally polarized photons,

$$R_g(x, Q^2, b) \approx 1 - \frac{\Delta\sigma_L^{\gamma^*p}(x, Q^2, b)}{T_A(b)\sigma_L^{\gamma^*p}(x, Q^2)}, \quad (23)$$

where  $\Delta\sigma_L^{\gamma^*p} = \sigma_L^{\gamma^*A} - A\sigma_L^{\gamma^*p}$  is the shadowing correction at impact parameter  $b$ , and  $\sigma_L^{\gamma^*p}(x, Q^2)$  is the total photoabsorption cross section for a longitudinal photon. The process with longitudinal photons is chosen because the aligned jets configurations are suppressed by powers of  $Q^2$ , so that the average size of the dipole is small,  $\langle r^2 \rangle \sim 1/Q^2$ , and nuclear shadowing mainly originates from gluons.

As it was shown in [54, 55],

$$\Delta\sigma_L^{\gamma^*p}(x, Q^2, b) = \int_{-\infty}^{+\infty} dz_1 \int_{-\infty}^{+\infty} dz_2 \Theta(z_2 - z_1) \rho_A(b, z_1) \rho_A(b, z_2) \Gamma(x, Q^2, z_2 - z_1), \quad (24)$$

where  $\rho_A(b, z)$  is the nuclear density, and  $\Gamma(x, Q^2, \Delta z)$  is defined as

$$\begin{aligned} \Gamma(x, Q^2, \Delta z) = & \Re \int_x^{0.1} \frac{d\alpha_G}{\alpha_G} \frac{16\alpha_{em} (\sum Z_q^2) \alpha_s(Q^2) C_{eff}^2}{3\pi^2 Q^2 \tilde{b}^2} \times \\ & \times [(1 - 2\zeta - \zeta^2) e^{-\zeta} + \zeta^2(3 + \zeta) E_1(\zeta)] \\ & \times \left[ \frac{t}{w} + \frac{\sinh(\Omega\Delta z)}{t} \ln\left(1 - \frac{t^2}{u^2}\right) + \frac{2t^3}{uw^2} + \frac{t \sinh(\Omega\Delta z)}{w^2} + \frac{4t^3}{w^3} \right], \end{aligned}$$

with

$$\begin{aligned} \tilde{b}^2 &= (0.65 GeV)^2 + \alpha_G Q^2, \\ \Omega &= \frac{iB}{\alpha_G(1 - \alpha_G)\nu}, \\ B &= \sqrt{\tilde{b}^4 - i\alpha_G(1 - \alpha_G)\nu C_{eff}\rho_A}, \\ \nu &= \frac{Q^2}{2m_N x}, \\ \zeta &= ixm_N \Delta z, \\ t &= \frac{B}{\tilde{b}^2}, \\ u &= t \cosh(\Omega\Delta z) + \sinh(\Omega\Delta z), \\ w &= (1 + t^2) \sinh(\Omega\Delta z) + 2t \cosh(\Omega\Delta z). \end{aligned}$$

Notice the importance of the  $Q$ -independent term in  $\tilde{b}^2$ , which controls the mean quark-gluon, or glue-gluon separation at low scale. The magnitude of this term dictated by various experimental data [63] and especially by data on diffraction [54], is rather large  $b_0^2 = (0.65 GeV)^2$ . This leads to a small dipole sizes  $r_0 \sim 0.3\text{fm}$  and weak gluon shadowing.

For heavy nuclei we may rely on the hard sphere approximation,  $\rho_A(r) \approx \rho_A(0)\Theta(R_A - r)$ , and simplify (24) to:

$$\Delta\sigma^{\gamma^*p}(x, Q^2, b) \approx \rho_A^2(0) \int_0^L d\Delta z (L - \Delta z) \Gamma(x, Q^2, \Delta z),$$

where  $L = 2\sqrt{R_A^2 - b^2}$ . For the total cross-section after integration over  $\int d^2b$  we get

$$\begin{aligned} \Delta\sigma^{\gamma^*p}(x, Q^2) &= \int d^2b \Delta\sigma^{\gamma^*p}(x, Q^2, b) \\ &\approx \frac{\pi\rho_A^2(0)}{12} \int_0^{2R} d\Delta z \Gamma(x, Q^2, \Delta z) (16R_A^3 - 12R_A^2\Delta z + \Delta z^3) \end{aligned}$$

The results of the evaluation of the gluon shadowing are presented in Section VII.

## VI. WAVE FUNCTIONS FROM THE INSTANTON VACUUM

In this section we present briefly some details of the evaluation of the photon wavefunction in the instanton vacuum model (see [56–58] and references therein). The central object of the model is the effective action for the light quarks in the instanton vacuum, which in the leading order in  $N_c$  has the form [57, 58]

$$S = \int d^4x \left( \frac{N}{V} \ln \lambda + 2\Phi^2(x) - \bar{\psi} (\hat{p} + \hat{v} - m - c\bar{L}f \otimes \Phi \cdot \Gamma_m \otimes fL) \psi \right),$$

where  $\Gamma_m$  is one of the matrices,  $\Gamma_m = 1, i\vec{\tau}, \gamma_5, i\vec{\tau}\gamma_5$ ,  $\psi$  and  $\Phi$  are the fields of constituent quarks and mesons respectively,  $N/V$  is the density of the instanton gas,  $\hat{v} \equiv v_\mu \gamma^\mu$  is the external vector current corresponding to the photon,  $L$  is the gauge factor,

$$L(x, z) = P \exp \left( i \int_z^x d\zeta^\mu v_\mu(\zeta) \right), \quad (25)$$

which provides the gauge covariance of the action, and  $f(p)$  is the Fourier transform of the zero-mode profile.

In the leading order in  $N_c$ , we have the same Feynman rules as in perturbative theory, but with a momentum-dependent quark mass  $\mu(p)$  in the quark propagator

$$S(p) = \frac{1}{\hat{p} - \mu(p) + i0}. \quad (26)$$

The mass of the constituent quark has a form

$$\mu(p) = m + M f^2(p),$$

where  $m \approx 5$  MeV is the current quark mass,  $M \approx 350$  MeV is the dynamical mass generated by the interaction with the instanton vacuum background. Due to the presence of the instantons the coupling of a vector current to a quark is also modified,

$$\begin{aligned} \hat{v} &\equiv v_\mu \gamma^\mu \rightarrow \hat{V} = \hat{v} + \hat{V}^{nonl}, \\ \hat{V}^{nonl} &\approx -2M f(p) \frac{df(p)}{dp_\mu} v_\mu(q) + \mathcal{O}(q^2). \end{aligned} \quad (27)$$

Notice that for an arbitrary photon momentum  $q$  the expression for  $\hat{V}^{nonl}$  depends on the choice of the path in (25) and as a result one can find in the literature different expressions used for evaluations [59–62]. In the limit  $p \rightarrow \infty$  the function  $f(p)$  falls off as  $\sim \frac{1}{p^3}$ , so for large  $p \gg \rho^{-1}$ , where  $\rho \approx (600 \text{ MeV})^{-1}$  is the mean instanton size, the mass of the quark  $\mu(p) \approx m$  and the vector current interaction vertex  $\hat{V} \approx \hat{v}$ . However, we would like to emphasize that the wavefunction  $\Psi(\beta, r)$  gets contributions from both the soft and the hard parts, so even in the large- $Q$  limit the instanton vacuum function is different from the well-known perturbative result.

We have to evaluate the wavefunctions associated with the following matrix elements:

$$I_\Gamma(\beta, \vec{r}) = \int \frac{dz^-}{2\pi} e^{i(\beta + \frac{1}{2})q^- z^+} \left\langle 0 \left| \bar{\psi} \left( -\frac{z}{2}n - \frac{\vec{r}}{2} \right) \Gamma \psi \left( \frac{z}{2}n + \frac{\vec{r}}{2} \right) \right| \gamma(q) \right\rangle, \quad (28)$$

where  $\Gamma$  is one of the matrices  $\Gamma = \gamma_\mu, \gamma_\mu \gamma_5, \sigma_{\mu\nu}$ . In the leading order in  $N_c$  one can easily obtain

$$I_\Gamma = \int \frac{d^4p}{(2\pi)^4} e^{i\vec{p}_\perp \cdot \vec{r}_\perp} \delta \left( p^+ - \left( \beta + \frac{1}{2} \right) q^+ \right) \text{Tr} \left( S(p) \hat{V} S(p+q) \Gamma \right). \quad (29)$$

The evaluation of (29) is quite tedious but straightforward. Details of this evaluation may be found in [59].

In what follows, we use Eqn (29) for the evaluation of the initial and final wavefunctions  $\Psi_{in,f}$ . Without any loss of generality, we may choose the frame with  $q = (M_\perp, 0, 0, 0)$  for the time-like photon, and the frame where  $q = (0, 0, 0, Q)$  for the space-like photon, and after that make a boost to the Bjorken frame. However, we would like to emphasize that application of (29) to the case of time-like photon should be done with care. Since the instanton vacuum model does not possess confinement, rigorously speaking Eq. (29) may be applied only if the virtuality is below the quark pair production threshold,  $M_\perp^2 \sim 4\mu^2(0) \sim m_\rho^2$  (in case of pQCD wave functions the corresponding

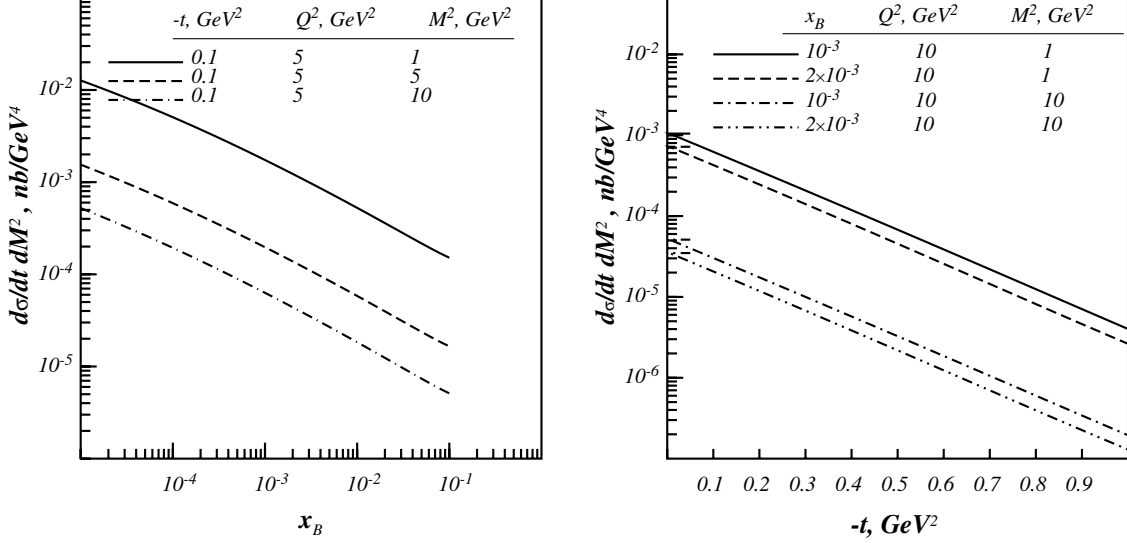


Figure 1: DDVCS cross-section on the proton. Left:  $x_B$ -dependence for different kinematical points. Right:  $t$ -dependence for different kinematical points.

threshold is located at  $M_{ll}^2 \sim 4m_q^2$ ). Such behavior is characteristic to all models which have quarks as degrees of freedom but do not have built-in confinement.

The overlap of the initial and final photon wavefunctions in (2) was evaluated according to

$$\Psi_f^{(i)*}(\beta, r, -M_{ll}^2) \Psi^{(i)}(\beta, r, Q^2) = \sum_{\Gamma} I_{\Gamma}^*(\beta, r^*, -M_{ll}^2) I_{\Gamma}(\beta, r, Q^2), \quad (30)$$

where the summation is over the possible polarization states  $\Gamma = \gamma_{\mu}, \gamma_{\mu}\gamma_5, \sigma_{\mu\nu}$ . In the final state we should use  $r_{\mu}^* = r_{\mu} + n_{\mu} \frac{q'_{\perp} \cdot r_{\perp}}{q_+} = r_{\mu} - n_{\mu} \frac{\Delta_{\perp} \cdot r_{\perp}}{q_+}$ , which is related to the reference frame with  $q'_{\perp} = 0$ , in which the components (29) were evaluated.

## VII. NUMERICAL RESULTS

In this section we present the results of numerical calculations. While currently there is no data for DDVCS, we expect that similar to DVCS the experiments will be done in the region of large virtualities  $Q^2$ . In that region we have Bjorken scaling, so all the model parameters such as basic cross-section  $\sigma_0$  and saturation radius  $R_0$  in Eq. (9). should depend on the Bjorken  $x_B$ . A widely accepted parameterization which incorporates this feature is the GBW-type parameterization [27, 36–38, 40]. The DDVCS cross-sections on the proton are shown in the Figure 1. Similar to DVCS, the DDVCS cross-section increases in the small- $x$  region like  $x^{\alpha}$ . As a function of  $t$ , the cross-section is exponentially decreasing.

The  $Q^2$ - and  $M^2$ -dependence of the DDVCS cross-section on the proton is shown in the Figure 2. As a function of the virtuality  $Q^2$ , the DDVCS cross-section weakly depends on  $Q^2$  for  $Q^2 \lesssim M_{ll}^2$ , but decreases like  $Q^{-4}$  for  $Q^2 \gg M_{ll}^2$ . Similar behavior is observed for  $M^2 d\sigma/dt dM^2$  for fixed  $Q^2$ . Physically, such behavior is clear: the average dipole size  $\langle r^2 \rangle$  is controlled by the wave function with largest virtuality, being  $\langle r^2 \rangle \sim 1/\max(Q^2, M_{ll}^2)$ .

As one can see from the Figure 3, the shadowing correction is increasing towards small  $x_B$ , and for  $x_B \sim 10^{-5}$  the nuclear cross-section ratio decreases by a factor of two compared to the naive estimate  $d\sigma_A \sim F_A^2(t) d\sigma_N$ . As a function of the momentum transfer  $t$ , the shadowing correction reveals a behavior qualitatively similar to the nuclear formfactor  $F_A(t)$ : it steeply drops at small- $t$  and has zeros for some  $t$ . Notice, however, that the zero positions in the cross-section do not coincide with the zeros of the formfactor. This is a result of shadowing which suppresses the contribution of the central part of the nucleus and modifies the  $b$ -dependence of the cross section compared to the formfactor.



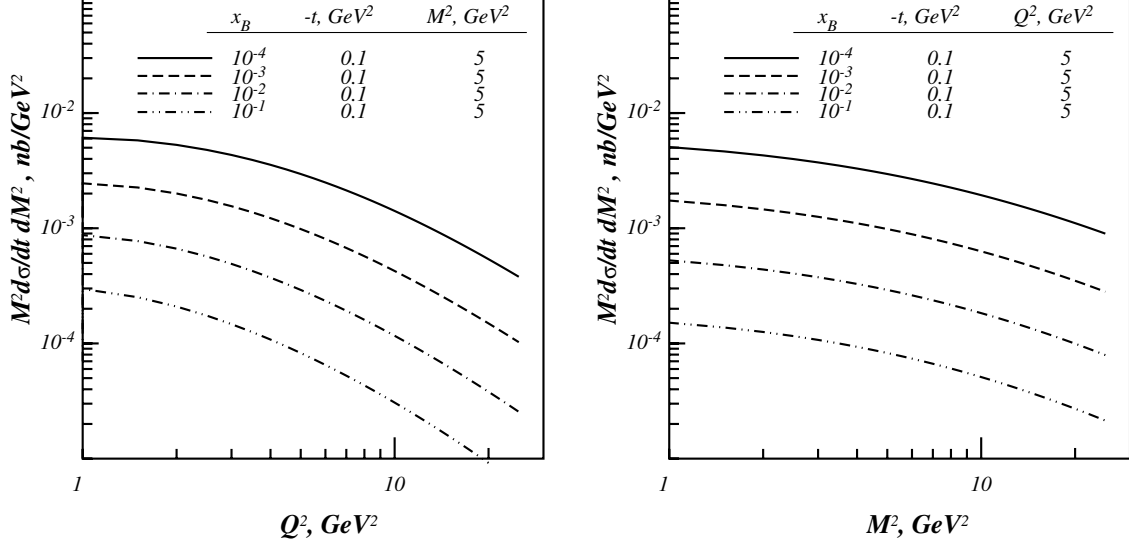


Figure 2: DDVCS cross-section on the proton. Here we plot  $M^2 d\sigma/dt dM^2$  instead of  $d\sigma/dt dM^2$  in order to hide the trivial  $1/M^2$  in Eq. (1). Left:  $Q^2$ -dependence for different kinematical points. Right:  $M^2$ -dependence for different kinematical points.

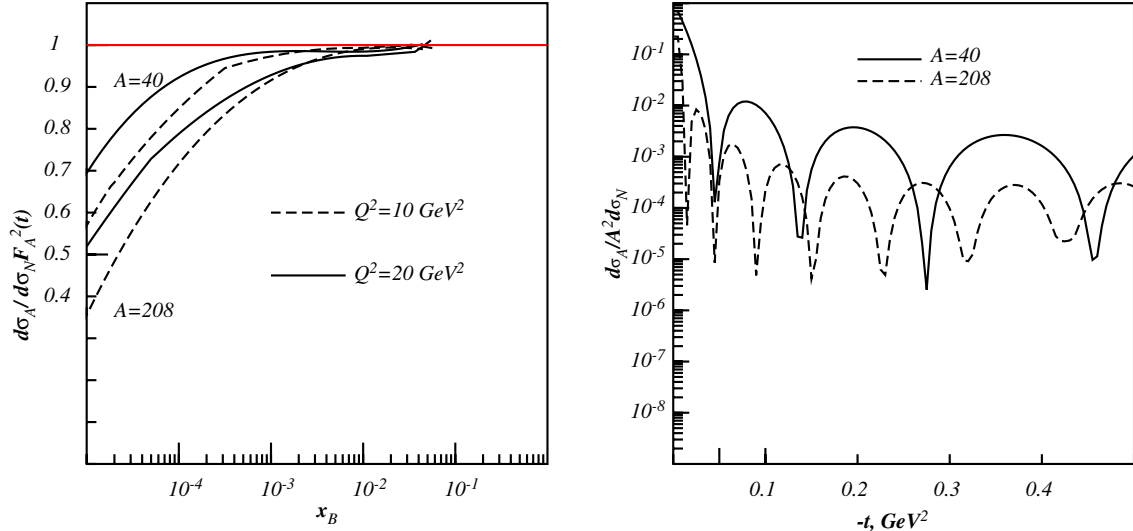


Figure 3: The nucleus to nucleon cross section ratio for the DDVCS as function of different kinematical variables. Left:  $x_B$ -dependence of the shadowing,  $t = t_{min}$ ,  $M_{ll}^2 = 10$  GeV<sup>2</sup>, for different  $Q^2$  and  $A$ . From top to bottom:  $A = 40$  and  $A = 208$ . Right:  $t$ -dependence,  $x_B = 10^{-3}$ ,  $M_{ll}^2 = 10$  GeV<sup>2</sup>.

The  $Q^2$ - and  $M^2$ -dependence of the shadowing is shown in the Figure 4. The  $Q^2$ -dependence is similar to the DVCS case: the shadowing ratio is homogeneously increasing and for asymptotically large  $Q^2$  reaches 1. The shadowing is also increasing as a function of  $M^2$ , but not so fast as a  $Q^2$ -dependence.

Concluding, we considered DDVCS on the proton and nuclear targets within the color dipole model. We found that the magnitude of the cross-section is small, of order a few picobarns, and thus requires accelerators with high luminosities (e.g. future electron-ion colliders EIC and LHeC, [21, 22]). The nuclear shadowing in the process is large and is important for analysis of DDVCS on nuclei.

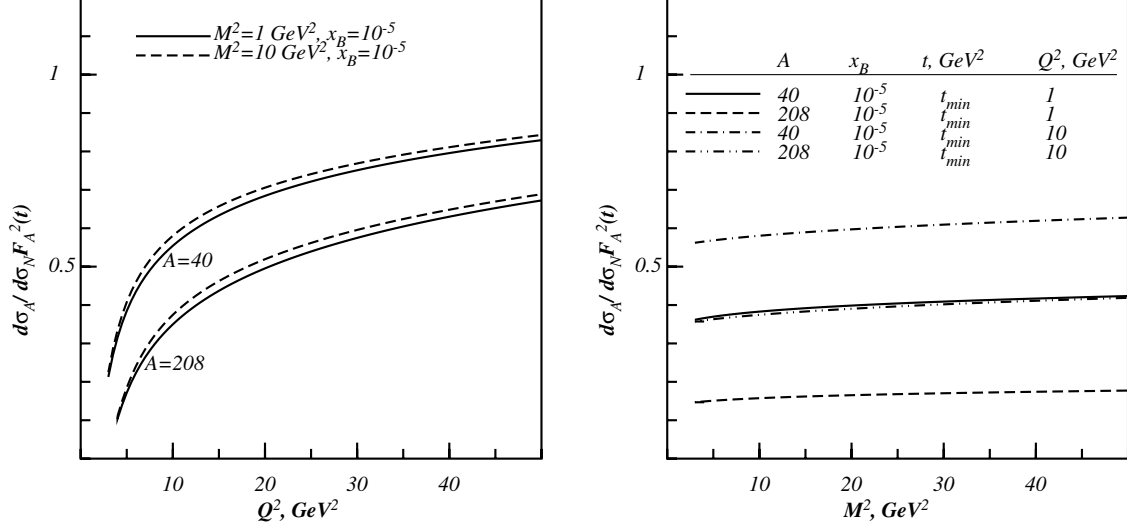


Figure 4: The nucleus to nucleon cross section ratio for the DDVCS as function of different kinematical variables. Left:  $Q^2$ -dependence,  $t = t_{min}$ ,  $x_B = 10^{-5}$  for different  $M_{il}^2$  and  $A$ . From top to bottom:  $A = 40$  and  $A = 208$ . Right:  $M^2$ -dependence for different kinematical variables.

### Acknowledgments

This work was supported in part by Fondecyt (Chile) grants 1090291, 1090073, 1100287, and by DFG (Germany) grant PI182/3-1.

- 
- [1] D. Mueller, D. Robaschik, B. Geyer, F. M. Dittes and J. Horejsi, Fortsch. Phys. **42**, 101 (1994) [arXiv:hep-ph/9812448].
  - [2] X. D. Ji, Phys. Rev. D **55**, 7114 (1997).
  - [3] X. D. Ji, J. Phys. G **24**, 1181 (1998) [arXiv:hep-ph/9807358].
  - [4] A. V. Radyushkin, Phys. Lett. B **380**, 417 (1996) [arXiv:hep-ph/9604317].
  - [5] A. V. Radyushkin, Phys. Rev. D **56**, 5524 (1997).
  - [6] A. V. Radyushkin, arXiv:hep-ph/0101225.
  - [7] S. Boffi and B. Pasquini, Riv. Nuovo Cim. **30** (2007) 387 [arXiv:0711.2625 [hep-ph]].
  - [8] X. D. Ji and J. Osborne, Phys. Rev. D **58** (1998) 094018 [arXiv:hep-ph/9801260].
  - [9] J. C. Collins and A. Freund, Phys. Rev. D **59** (1999) 074009 [arXiv:hep-ph/9801262].
  - [10] J. C. Collins, L. Frankfurt and M. Strikman, Phys. Rev. D **56**, 2982 (1997).
  - [11] S. J. Brodsky, L. Frankfurt, J. F. Gunion, A. H. Mueller and M. Strikman, Phys. Rev. D **50**, 3134 (1994).
  - [12] K. Goeke, M. V. Polyakov and M. Vanderhaeghen, Prog. Part. Nucl. Phys. **47**, 401 (2001) [arXiv:hep-ph/0106012].
  - [13] M. Diehl, T. Feldmann, R. Jakob and P. Kroll, Nucl. Phys. B **596**, 33 (2001) [Erratum-ibid. B **605**, 647 (2001)] [arXiv:hep-ph/0009255].
  - [14] A. V. Belitsky, D. Mueller and A. Kirchner, Nucl. Phys. B **629**, 323 (2002) [arXiv:hep-ph/0112108].
  - [15] M. Diehl, Phys. Rept. **388**, 41 (2003) [arXiv:hep-ph/0307382].
  - [16] A. V. Belitsky and A. V. Radyushkin, Phys. Rept. **418**, 1 (2005) [arXiv:hep-ph/0504030].
  - [17] V. P. Goncalves, M. V. T. Machado and A. R. Meneses, arXiv:1003.0828 [hep-ph].
  - [18] M. Guidal and M. Vanderhaeghen, Phys. Rev. Lett. **90** (2003) 012001 [arXiv:hep-ph/0208275].
  - [19] A. V. Belitsky and D. Mueller, Phys. Rev. Lett. **90** (2003) 022001 [arXiv:hep-ph/0210313].
  - [20] A. V. Belitsky and D. Mueller, Phys. Rev. D **68** (2003) 116005 [arXiv:hep-ph/0307369].
  - [21] M. Klein *et al.*, In the Proceedings of 11th European Particle Accelerator Conference (EPAC 08), Magazzini del Cotone, Genoa, Italy, 23-27 Jun 2008, pp WEOAG01.
  - [22] F. Zimmermann *et al.*, In the Proceedings of 11th European Particle Accelerator Conference (EPAC 08), Magazzini del Cotone, Genoa, Italy, 23-27 Jun 2008, pp WEPP154.
  - [23] E. R. Berger, M. Diehl and B. Pire, Eur. Phys. J. C **23** (2002) 675 [arXiv:hep-ph/0110062].
  - [24] B. Pire, L. Szymanowski and J. Wagner, Phys. Rev. D **79** (2009) 014010 [arXiv:0811.0321 [hep-ph]].
  - [25] M. V. T. Machado, Phys. Rev. D **78** (2008) 034016 [arXiv:0805.3144 [hep-ph]].

- [26] B. Z. Kopeliovich, I. Schmidt and M. Siddikov, Phys. Rev. D **79** (2009) 034019 [arXiv:0812.3992 [hep-ph]].
- [27] B. Z. Kopeliovich, I. Schmidt and M. Siddikov, Phys. Rev. D **80** (2009) 054005 [arXiv:0906.5589 [hep-ph]].
- [28] M. V. T. Machado, Eur. Phys. J. C **59** (2009) 769 [arXiv:0810.3665 [hep-ph]].
- [29] M. V. T. Machado, arXiv:0905.4516 [hep-ph].
- [30] B. Z. Kopeliovich, I. Schmidt and M. Siddikov, Phys. Rev. D **81** (2010) 094013 [arXiv:1003.4188 [hep-ph]].
- [31] V. N. Gribov, Sov. Phys. JETP **29** (1969) 483 [Zh. Eksp. Teor. Fiz. **56** (1969) 892].
- [32] R. J. Glauber, Phys. Rev. **100** (1955) 242.
- [33] J. B. Kogut and D. E. Soper, Phys. Rev. D **1** (1970) 2901.
- [34] J. D. Bjorken, J. B. Kogut and D. E. Soper, Phys. Rev. D **3** (1971) 1382.
- [35] L. Motyka and G. Watt, Phys. Rev. D **78** (2008) 014023 [arXiv:0805.2113 [hep-ph]].
- [36] B. Z. Kopeliovich, H. J. Pirner, A. H. Rezaeian and I. Schmidt, Phys. Rev. D **77** (2008) 034011 [arXiv:0711.3010 [hep-ph]].
- [37] B. Z. Kopeliovich, A. H. Rezaeian and I. Schmidt, arXiv:0809.4327 [hep-ph], to appear in Phys. Rev. D.
- [38] B. Z. Kopeliovich, I. K. Potashnikova, I. Schmidt and J. Soffer, Phys. Rev. D **78** (2008) 014031 [arXiv:0805.4534 [hep-ph]].
- [39] P. V. Pobylitsa, Phys. Rev. D **65** (2002) 114015 [arXiv:hep-ph/0201030].
- [40] K. J. Golec-Biernat and M. Wüsthoff, Phys. Rev. D **59** (1999) 014017 [arXiv:hep-ph/9807513].
- [41] B. Z. Kopeliovich, L. I. Lapidus and A. B. Zamolodchikov, JETP Lett. **33** (1981) 595 [Pisma Zh. Eksp. Teor. Fiz. **33** (1981) 612].
- [42] J. B. Bronzan, G. L. Kane and U. P. Sukhatme, Phys. Lett. B **49** (1974) 272.
- [43] J. D. Bjorken and J. B. Kogut, Phys. Rev. D **8**, 1341 (1973).
- [44] B. Z. Kopeliovich, J. Raufeisen and A. V. Tarasov, Phys. Rev. C **62**, 035204 (2000).
- [45] B. Z. Kopeliovich, I. K. Potashnikova and I. Schmidt, Phys. Rev. C **73**, 034901 (2006).
- [46] B. Z. Kopeliovich, J. Raufeisen and A. V. Tarasov, **440** (1998) 151 [arXiv:hep-ph/9807211].
- [47] B. Z. Kopeliovich and B. G. Zakharov, Phys. Rev. D **44**, 3466 (1991).
- [48] J. Nemchik, Phys. Rev. C **68**, 035206 (2003) [arXiv:hep-ph/0301043].
- [49] B. Kopeliovich and B. Povh, Phys. Lett. B **367**, 329 (1996); Z. Phys. A **356**, 467 (1997) [arXiv:nucl-th/9607035].
- [50] O. V. Kancheli, Pisma Zh. Eksp. Teor. Fiz. **18** (1973) 465.
- [51] L. V. Gribov, E. M. Levin and M. G. Ryskin, Phys. Rept. **100** (1983) 1.
- [52] F. Arleo and T. Gousset, Phys. Lett. B **660** (2008) 181 [arXiv:0707.2944 [hep-ph]].
- [53] N. Armesto, J. Phys. G **32** (2006) R367 [arXiv:hep-ph/0604108].
- [54] B.Z. Kopeliovich, A. Schäfer and A.V. Tarasov, Phys. Rev. D **62**, 054022 (2000).
- [55] B. Z. Kopeliovich, J. Raufeisen, A. V. Tarasov and M. B. Johnson, Phys. Rev. C **67** (2003) 014903 [arXiv:hep-ph/0110221].
- [56] T. Schafer and E. V. Shuryak, Rev. Mod. Phys. **70** (1998) 323 [arXiv:hep-ph/9610451].
- [57] D. Diakonov and V. Y. Petrov, Nucl. Phys. B **272** (1986) 457
- [58] D. Diakonov, M. V. Polyakov and C. Weiss, Nucl. Phys. B **461** (1996) 539 [arXiv:hep-ph/9510232].
- [59] A. E. Dorokhov, W. Broniowski and E. Ruiz Arriola, Phys. Rev. D **74** (2006) 054023 [arXiv:hep-ph/0607171].
- [60] I. V. Anikin, A. E. Dorokhov and L. Tomio, Phys. Part. Nucl. **31** (2000) 509 [Fiz. Elem. Chast. Atom. Yadra **31** (2000) 1023].
- [61] A. E. Dorokhov and W. Broniowski, Eur. Phys. J. C **32** (2003) 79 [arXiv:hep-ph/0305037].
- [62] K. Goetze, M. M. Musakhanov and M. Siddikov, Phys. Rev. D **76** (2007) 076007 [arXiv:0707.1997 [hep-ph]].
- [63] B. Z. Kopeliovich, I. K. Potashnikova, B. Povh and I. Schmidt, **76**, 094020 (2007).
- [64] K. J. Eskola, H. Paukkunen and C. A. Salgado, JHEP **0807**, 102 (2008) [arXiv:0802.0139 [hep-ph]].
- [65] B. Z. Kopeliovich, E. Levin, I. K. Potashnikova and I. Schmidt, **79**, 064906 (2009) [arXiv:0811.2210 [hep-ph]].